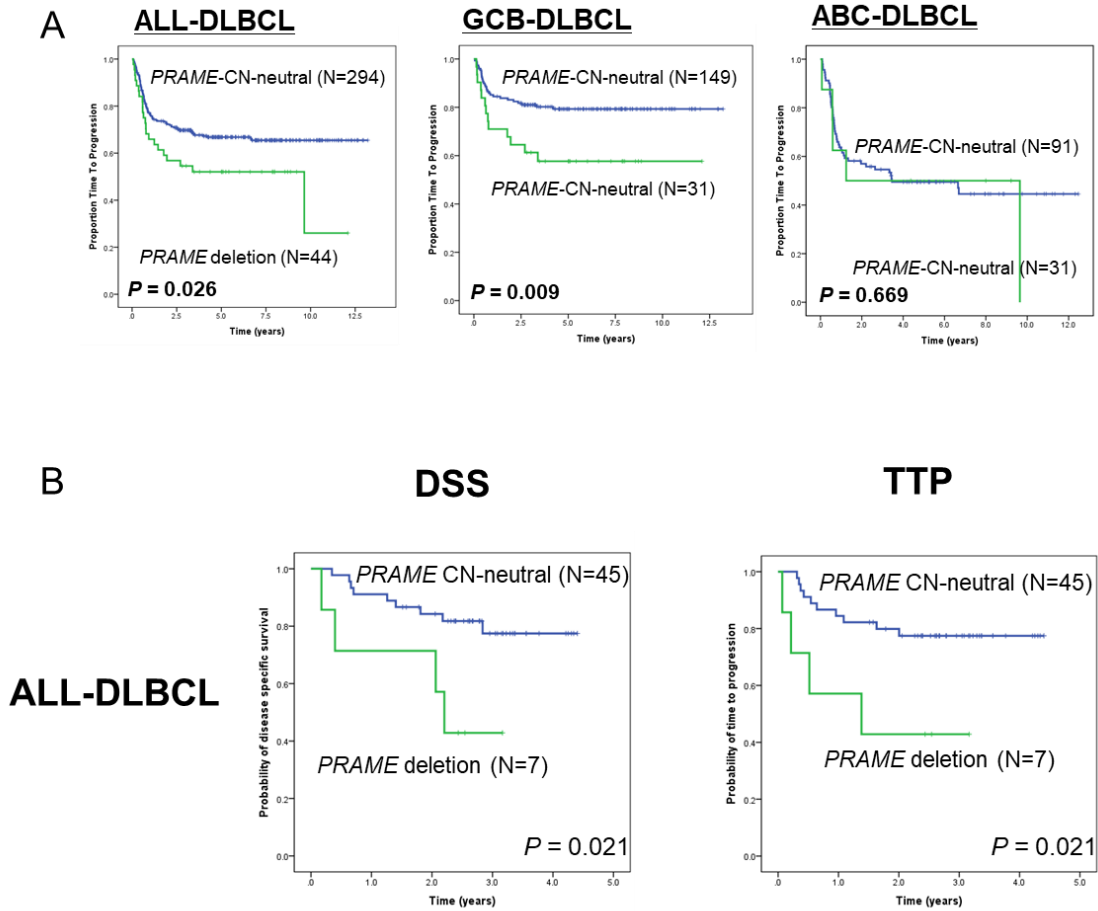


## Supplementary Materials

### **The tumor associated antigen PRAME exhibits dualistic functions that are targetable in diffuse large B cell lymphoma**

Katsuyoshi Takata<sup>1,2</sup>, Lauren C. Chong<sup>1</sup>, Daisuke Ennishi<sup>1</sup>, Tomohiro Aoki<sup>1</sup>, Michael Yu Li<sup>1</sup>, Avinash Thakur<sup>3,4</sup>, Shannon Healy<sup>1</sup>, Elena Viganò<sup>1</sup>, Tao Dao<sup>5</sup>, Daniel Kwon<sup>6</sup>, Gerben Duns<sup>1</sup>, Julie S. Nielsen<sup>7</sup>, Susana Ben-Neriah<sup>1</sup>, Ethan Tse<sup>1</sup>, Stacy Hung<sup>1</sup>, Merrill Boyle<sup>1</sup>, Sung Soo Mun<sup>5</sup>, Christopher Bourne<sup>5</sup>, Bruce Woolcock<sup>1</sup>, Adèle Telenius<sup>1</sup>, Makoto Kishida<sup>1</sup>, Shinya Rai<sup>1</sup>, Allen Zhang<sup>8</sup>, Ali Bashashati<sup>8</sup>, Saeed Saberi<sup>8</sup>, Gianluca D'Antonio<sup>7</sup>, Brad H. Nelson<sup>7</sup>, Sohrab P. Shah<sup>8,9</sup>, Pamela A. Hoodless<sup>3,4</sup>, Ari M. Melnick<sup>10</sup>, Randy D. Gascoyne<sup>1</sup>, Joseph M. Connors<sup>1</sup>, David A. Scheinberg<sup>5</sup>, Wendy Béguelin<sup>10</sup>, David W. Scott<sup>1</sup>, Christian Steidl<sup>1,11\*</sup>

Correspondence to: [CSteidl@bccancer.bc.ca](mailto:CSteidl@bccancer.bc.ca)

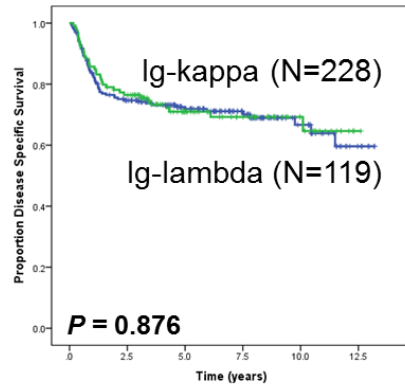


**Figure.S1. Kaplan-Meier analysis of discovery cohort and validation cohort. (A)** Time to Progression (TTP) survival in all- (left), GCB- (middle), and ABC-DLBCL (right). (B) Disease specific survival (DSS) and TTP in all-DLBCL in an independent DLBCL cohort (n=52).

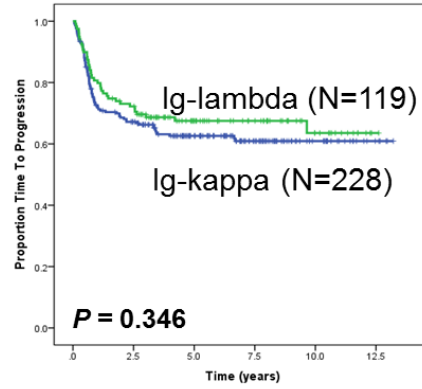
A

**ALL-DLBCL**

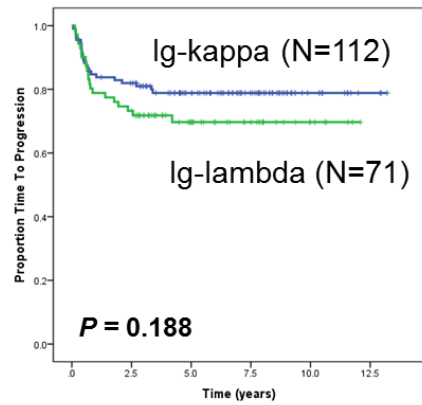
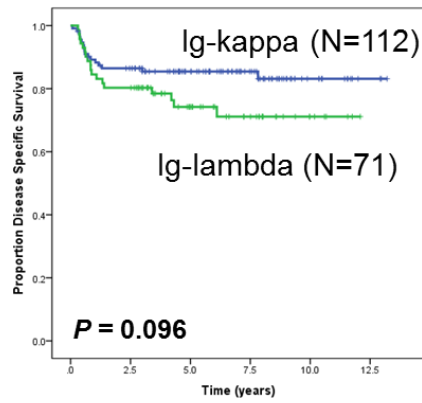
**DSS**

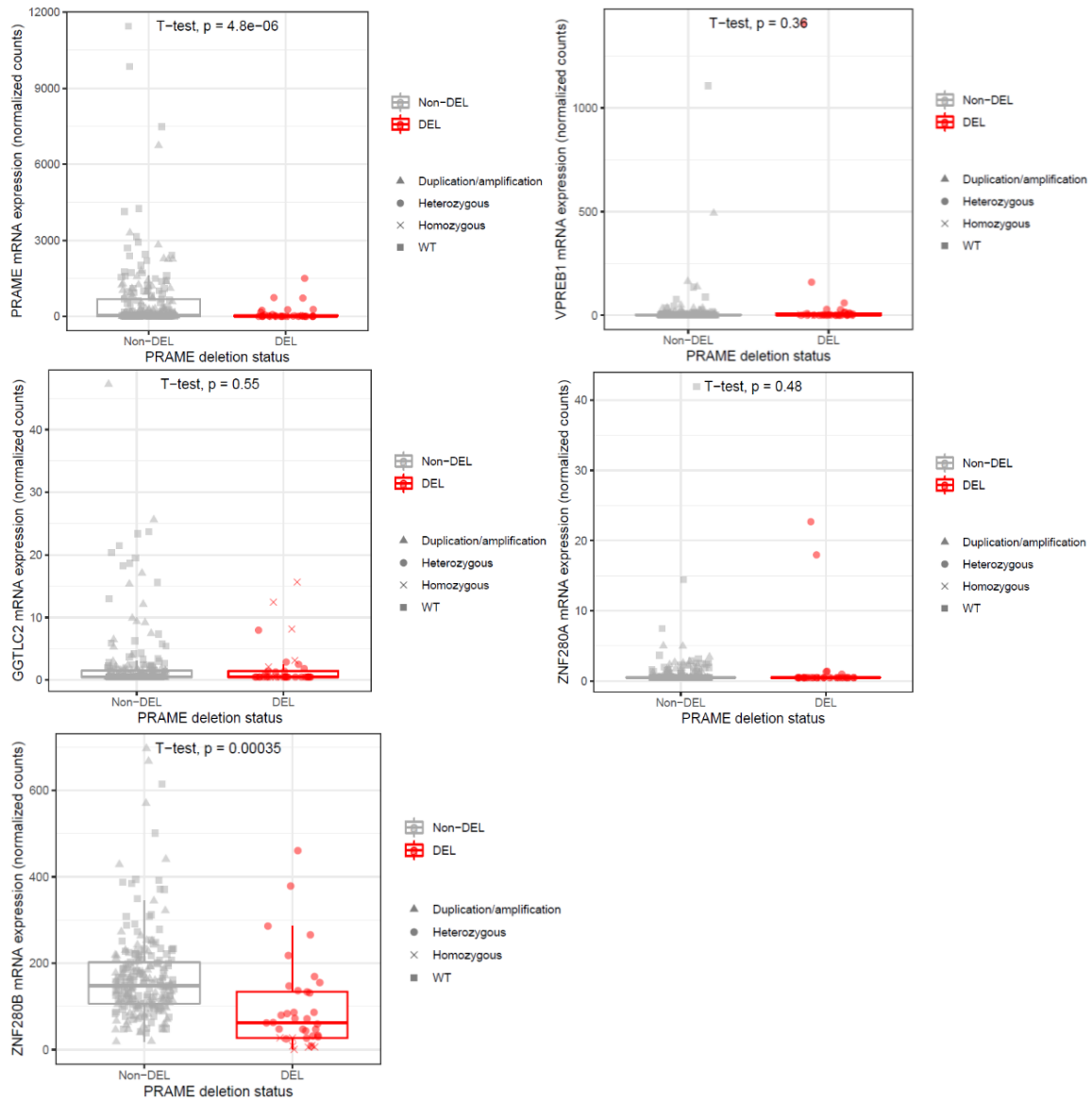


**TTP**

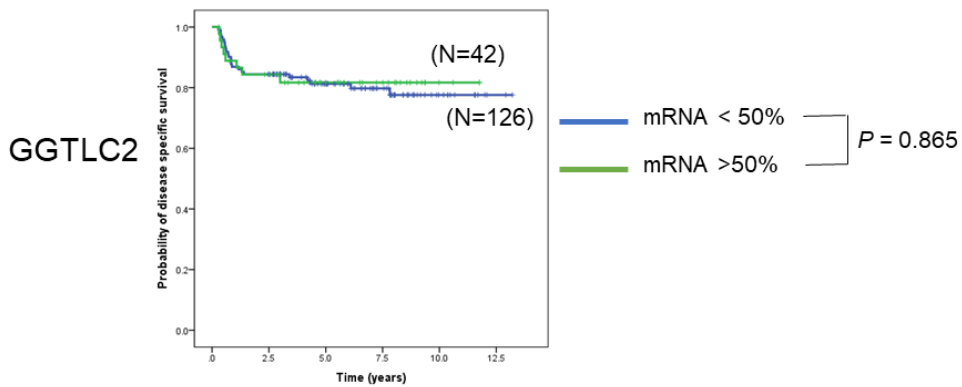
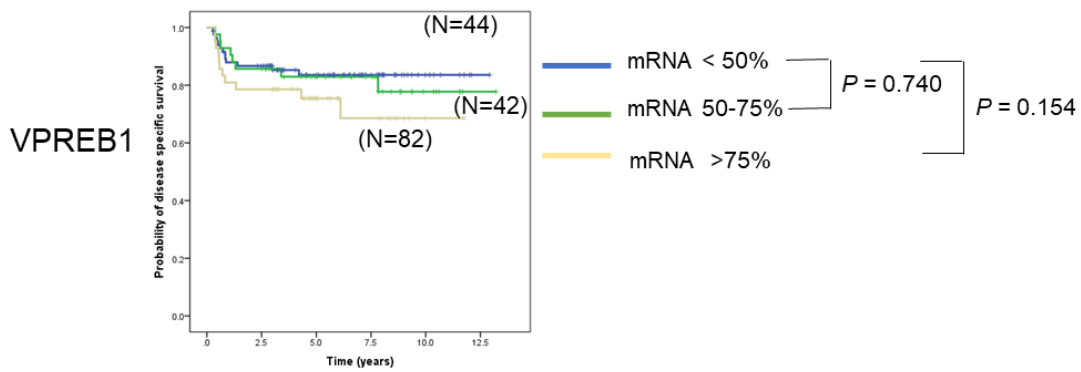
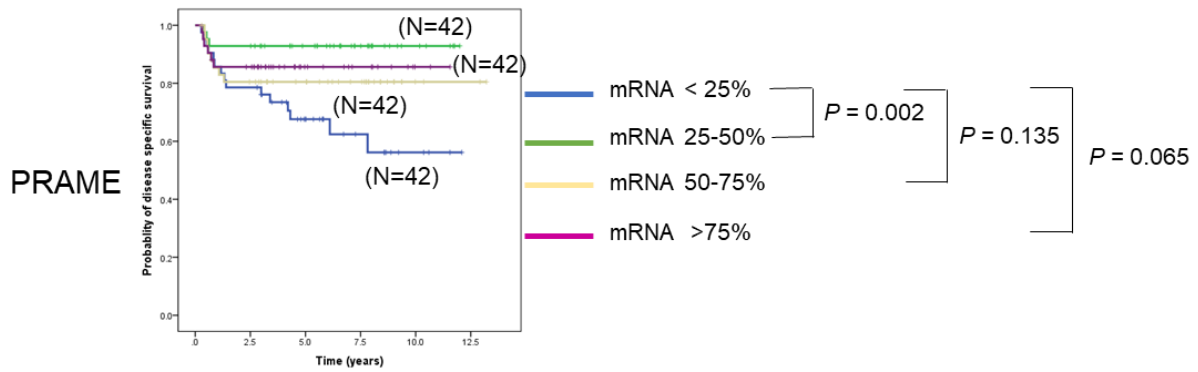


**GCB-DLBCL**



**B**

C



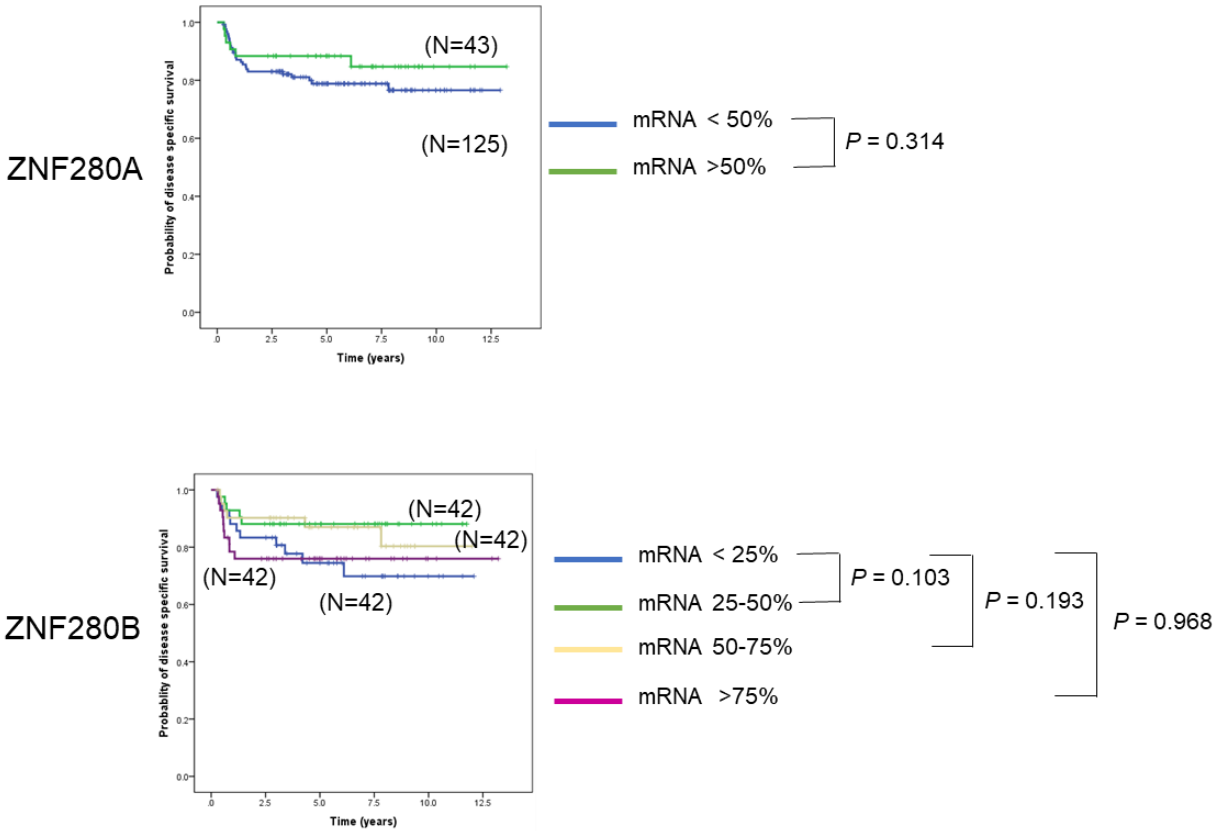
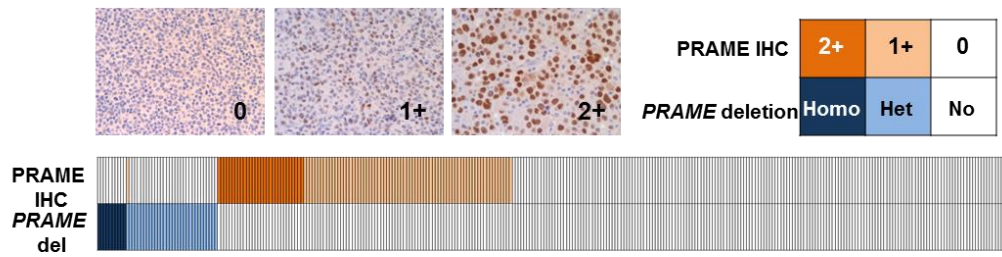


**Figure. S2. Correlation analysis for the Ig-lambda and 5 genes involved in 22q11.22 deletion area.**

(A) Kaplan-Meier curves represent DSS and TTP survival according to Ig-rearrangement status in all- (upper) and GCB-DLBCL (lower). (B) Cis-correlation analysis of mRNA for 5 genes (*PRAME*, *GGTCL2*, *VPREB1*, *ZNF280A*, *ZNF280B*) with *PRAME* deletion status. (C) Outcome correlation analysis using unbiased quartile mRNA cut-offs (25%, 50%, and 75%). Less than 25% of mRNA were included into <50% in *VPREB1*, *GGTCL2*, and *ZNF280A* because samples in the <25% and <50% quartiles showed same expression value.

A



B

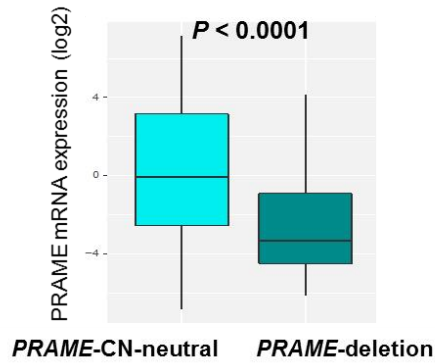


**Figure.S3. Correlation with Ig-kappa, -lambda, immunohistochemistry, and mRNA.** (A) Representative immunohistochemistry of PRAME and correlation with *PRAME* genetic status. (B) Correlation between *PRAME* deletion status and PRAME mRNA expression.

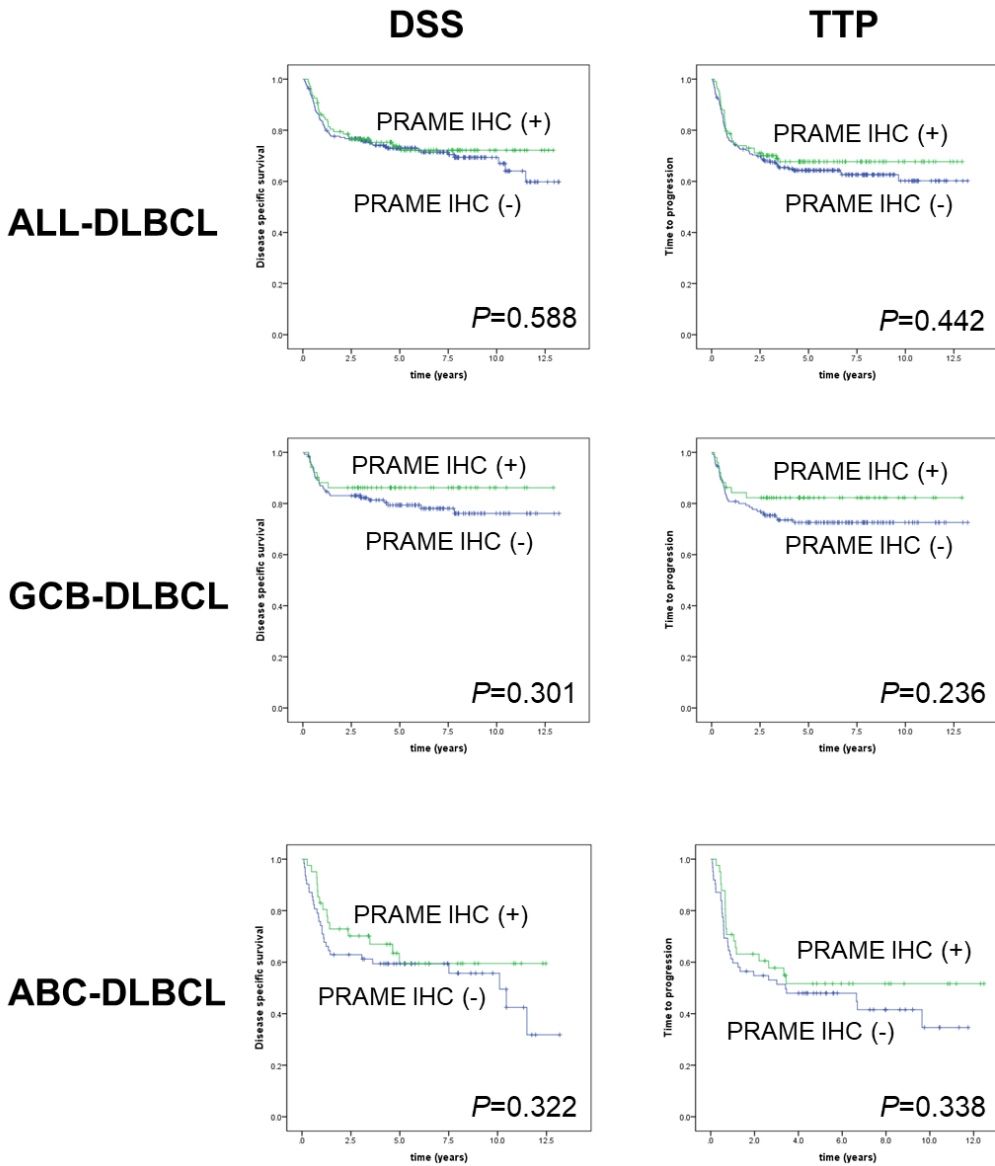
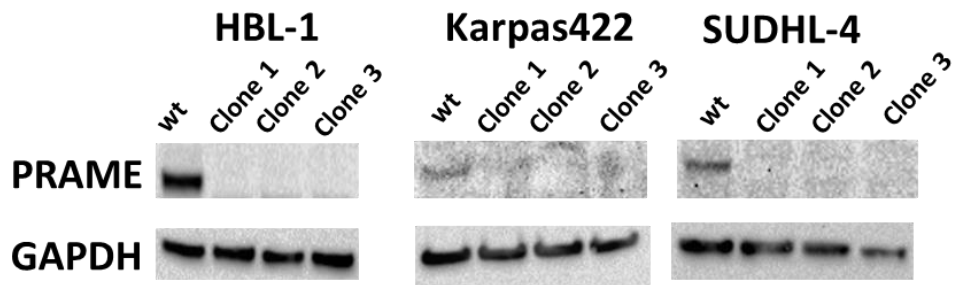


**Figure.S4. Outcome correlation with PRAME IHC status.**

Kaplan-Meier curves represent DSS and TTP survival according to PRAME IHC status in all- (upper), GCB- (middle), and ABC-DLBCL (lower).



A

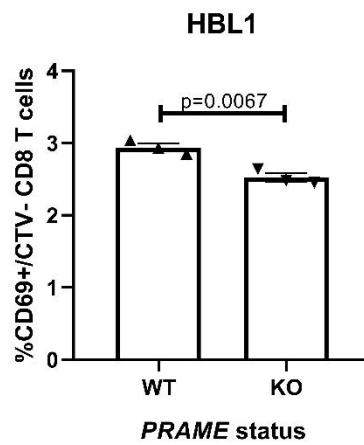
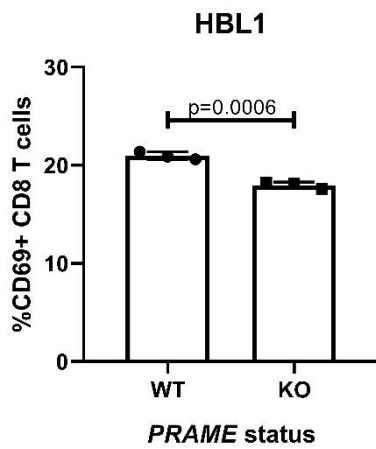
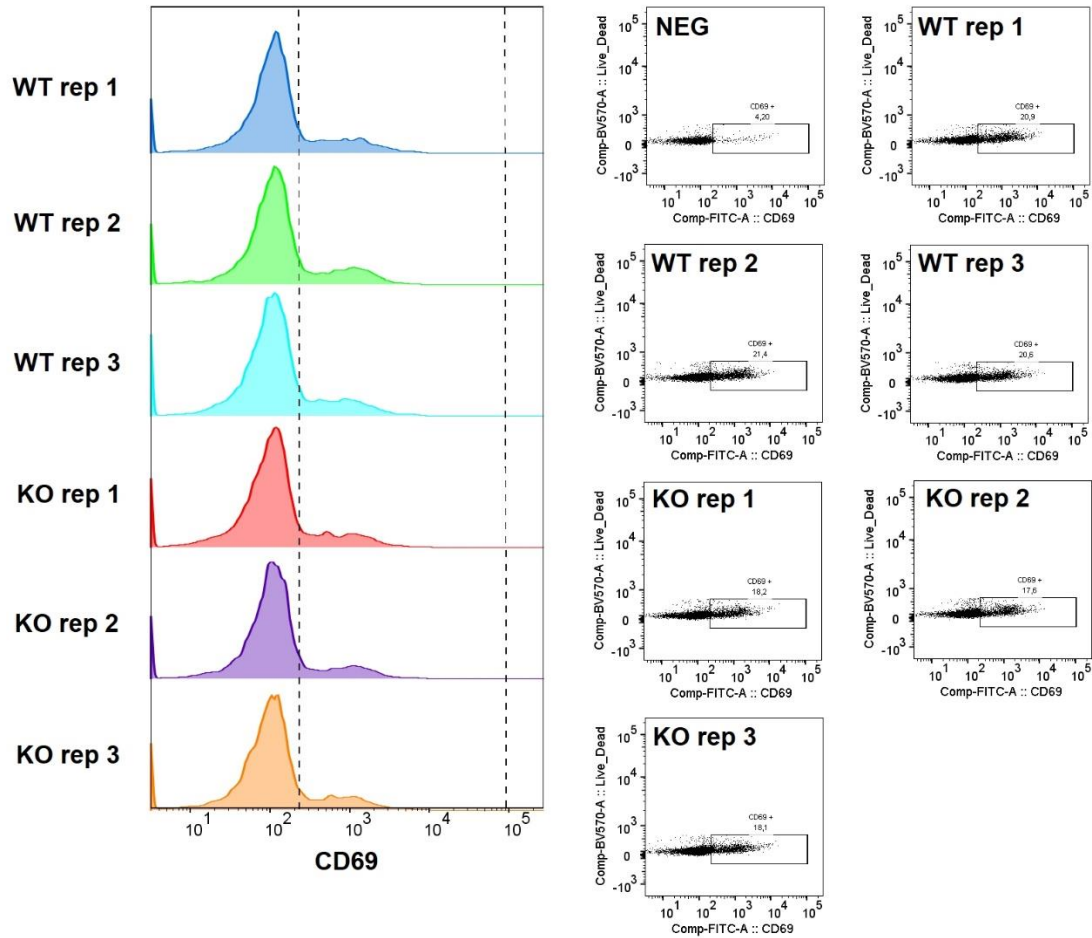


B

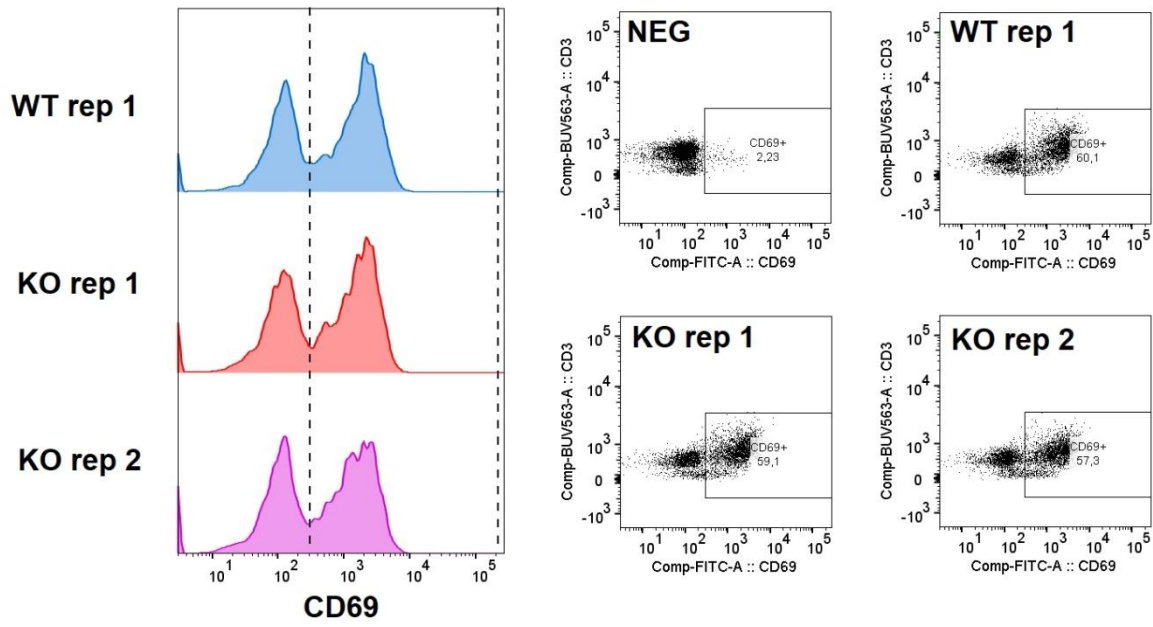
Cell line and clone	Sequence	Description
HBL-1 clone 1	TGTGgacaagcccacggagacttgGAGC	22bp frameshift
	CCCtctgtgtgctagcac agtgactttggccctaagttggtccct	177bp frameshift
	cagaagggtaggaaaagatagagttgcttatgcttgggctgaaag	
	ggatgcctgttcctgtatgttctcagggttcattcagagccgatacat	
	cagcatgagtgtgtggacaagcccacggagacttg tggagctggcagggcagagcCTGCT	
HBL-1 clone 2	AAGtctccgtggGCTTGT	9bp frameshift
	AGCTcacaagtctccgtgggcttgcCACACA	22bp frameshift
HBL-1 clone 3	GTCTCcgtagggcTTGTCC	7bp frameshift
	GCAGGctctgcccctgccagctccacaagtctccgt	238bp frameshift
	gggctgtccacacactcatgctgatgtatcggctctgaatggaaccctg	
	aggaaacatacagggaaacaaggcatcccttcagcccagcataagcaac	
	tctatcttttctcaccctctgagggaccaacttagggccaaagtcact tgctagcaacagcaggggagttctAGTTTA	
Karpas-422 clone 1	CCAgctccacaagtctccgtggGCTTGTCC	19bp frameshift
	CCAGCTCCAC AAGTctccGTGGGCT	4bp frameshift
Karpas-422 clone 2	CAAgctccGTGGGCTTGTCC	6bp frame shift
	CAAgctccGTGGGCTTGTCC	6bp frame shift
Karpas422 clone 3	CCAgctccacaagtctccgtggGCTTGTCC	19bp frameshift
	CCAgctccacaagtctccgtggGCTTGTCC	19bp frameshift
SU-DHL-4 clone 1	AAGTctccgtgggcttgtccacacactcatgctgatgtatcggctctg	113bp frameshift
	aatggaaccctgaggaaacatacagggaaacaaggcatccctt	
	cagccaagcataagcaCTCT TGCcagctccacaagtctccgtgggcttgcCACA	28bp frameshift
SU-DHL-4 clone 2	TGCcagctccacaagtctccgtgggcttgcCACA	28bp frameshift
	TGCcagctccacaagtctccgtgggcttgcCACA	28bp frameshift
SU-DHL-4 clone 3	AGAGggaggcaggtgaagGGCC	14bp frameshift
	AACTTA <sub>g</sub> GGCCAA	1bp frameshift

**Figure S5. Western Blotting and Sanger sequencing results for PRAME isogenic knockout clones in DLBCL cell lines. (A) Western Blotting of PRAME and GAPDH. Protein lysate (for anti-PRAME: 20µg, for anti-GAPDH: 5µg) was loaded in the separate gels and transferred to separate membranes. (B) Summary of Sanger sequencing for PRAME exon 4 region.**

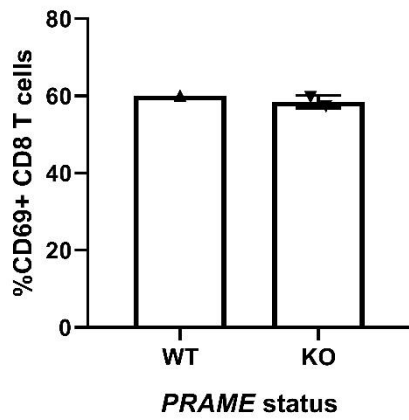
A



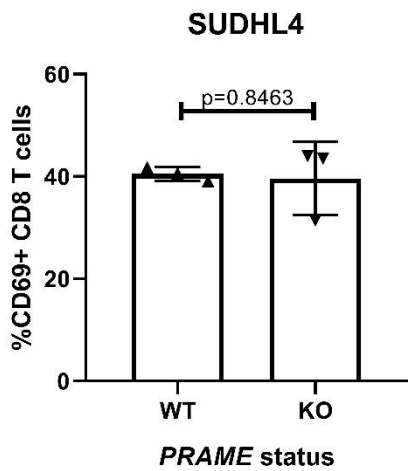
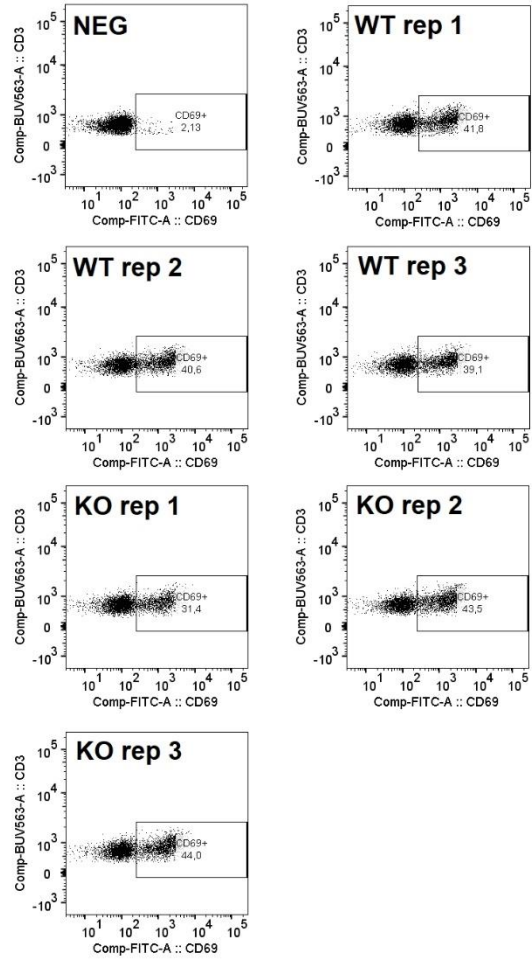
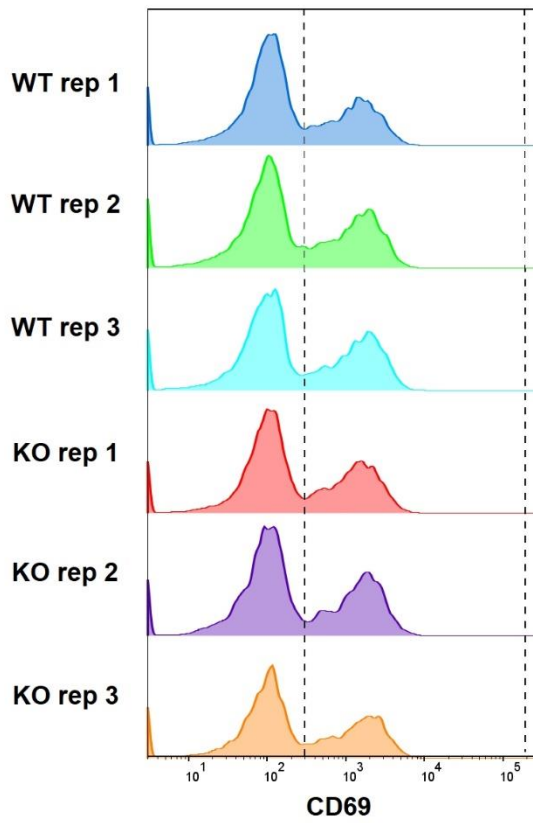
B



**Karpas422**



C



D

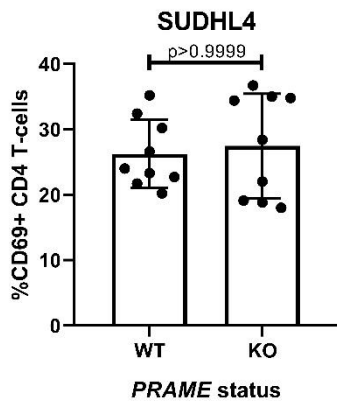
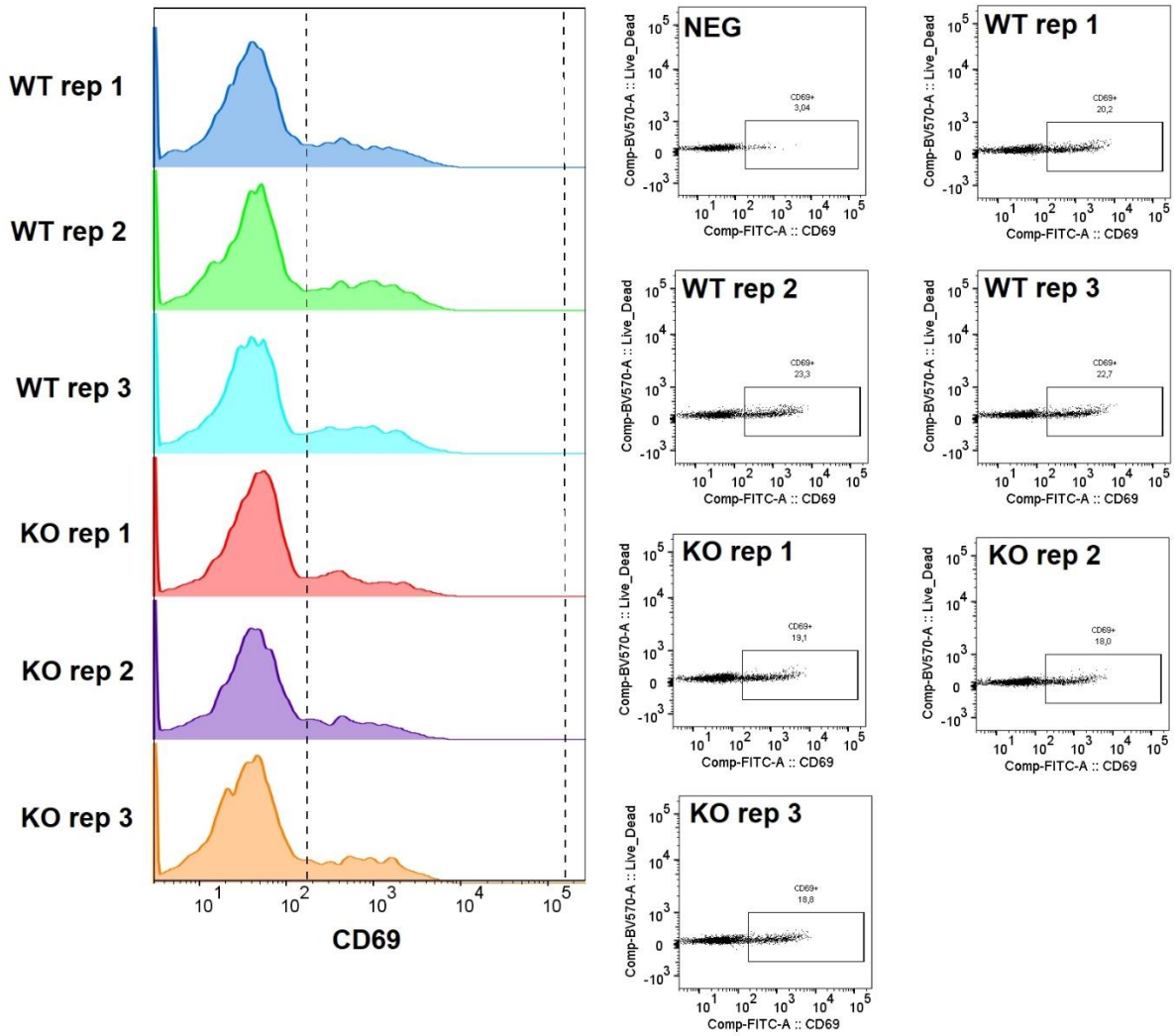


**Figure S6. Co-culture analysis on SU-DHL-4 and HBL-1 cells**

- (A) CD69+ CD8 T-cell populations (upper: FACS plot, lower left: bar-graph for CD69+ population, lower right: CD69+ CTV population) for co-cultured with HBL-1 PRAME isogenic cell lines.
- (B) CD69+ CD8 T-cell populations (upper: FACS plot, lower: bar-graph) for co-cultured with Karpas-422 PRAME isogenic cell lines.
- (C) CD69+ CD8 T-cell populations (upper: FACS plot, lower: bar-graph) for co-cultured with SU-DHL-4 PRAME isogenic cell lines.
- (D) CD69+ CD4 T-cell populations (upper: FACS plot, lower: bar-graph) for co-cultured with SU-DHL-4 PRAME isogenic cell lines.

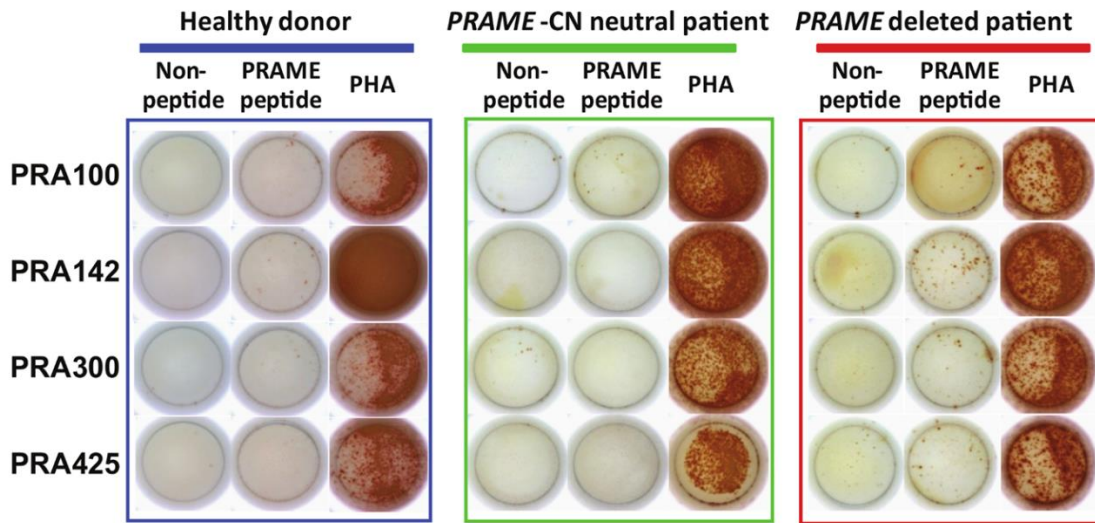
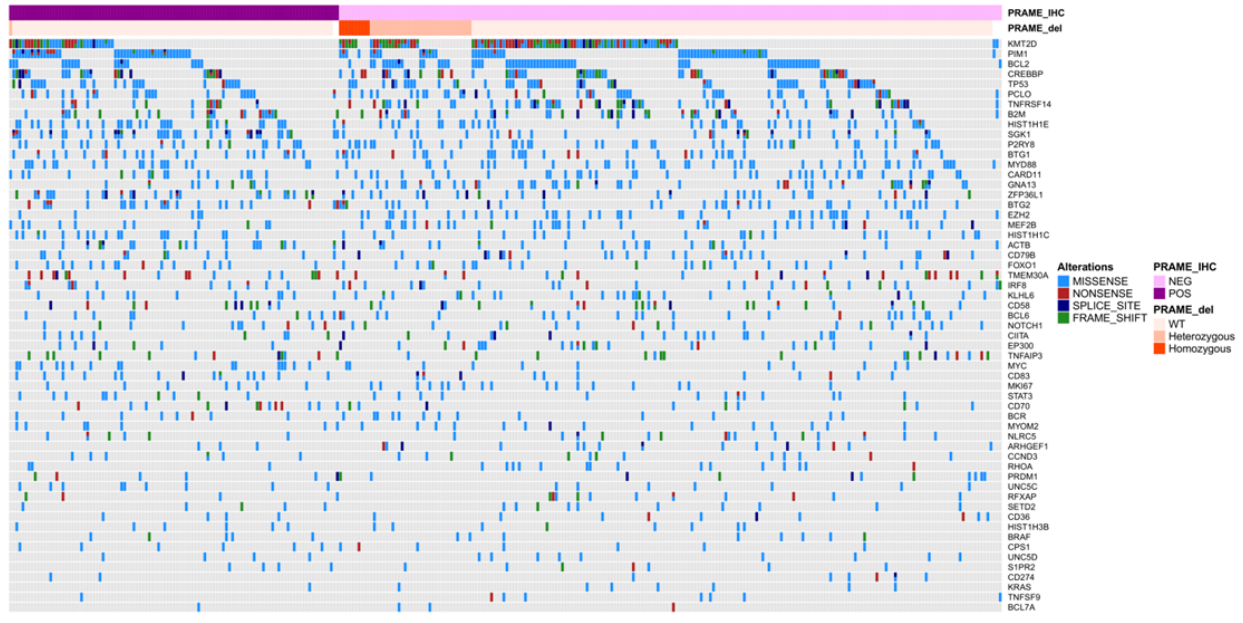
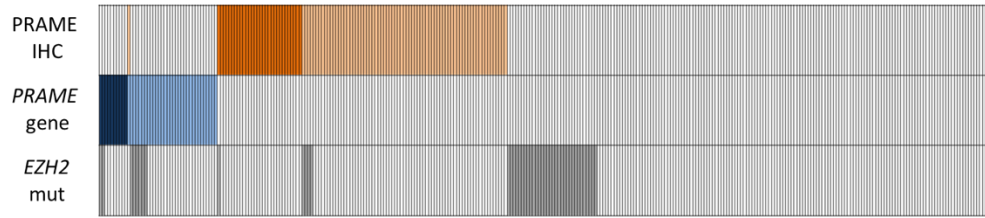


Figure. S7. Representative IFN  $\gamma$  ELISPOT assay results of healthy donor, *PRAME* CN-neutral, and *PRAME* deleted patient derived T-cells.





**Figure.S8. Mutation oncoprint between PRAME IHC-negative and IHC-positive samples.**



EZH2mut vs PRAME IHC

$P = 0.0009$  (correlation value 0.185) Pearson's correlation test

	PRAME IHC		
	2+	1+	0
PRAME gene deletion	Homo	Hetero	No
EZH2 mutation	+	-	

	PRAME-CN-neutral	PRAME-deleted
EZH2-mut	37	8
EZH2-wt	257	36

Fisher exact test:  $P = 0.3398$

**Figure S9. Correlation among PRAME-IHC status, PRAME-CN, and EZH2-mutation.**

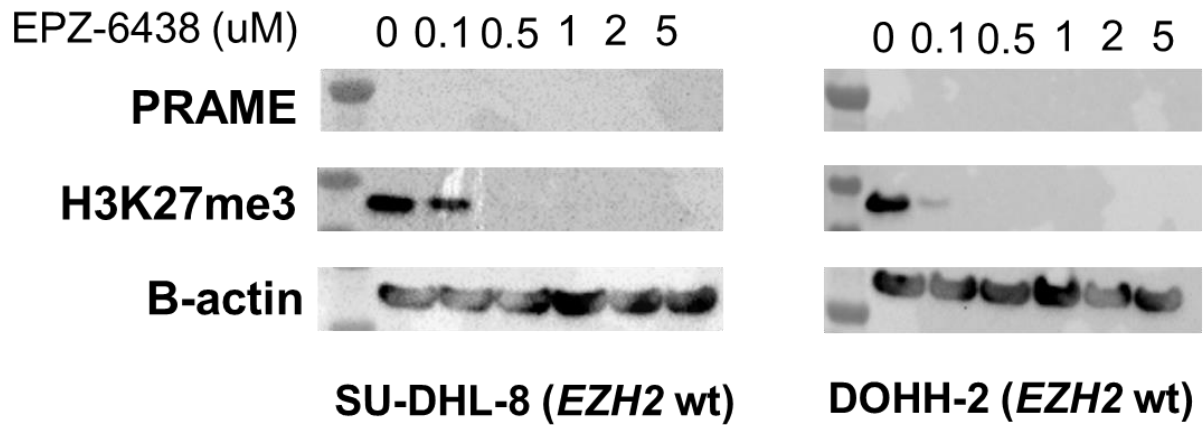


**Figure. S10. Immunoblot for EPZ-6438 treated cells (*EZH2* wt).**  
**Protein lysate (anti-PRAME and anti-H3K27me3: 20µg, anti-B-actin: 20µg) was loaded in the separate gels and transferred to separate membranes).**

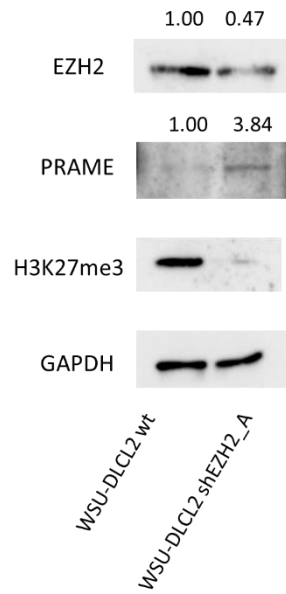


**Figure. S11. EZH2, PRAME, H3K27me3 and GAPDH Immunoblot for EZH2 knock-down by shEZH2 system. Protein lysate (anti-EZH2, anti-PRAME, anti-H3K27me3: 20 $\mu$ g, anti-GAPDH: 5 $\mu$ g) was loaded in the separate gels and transferred to separate membranes. Detecting anti-PRAME membrane was visualized using high-sensitivity chemiluminescent reagent.**

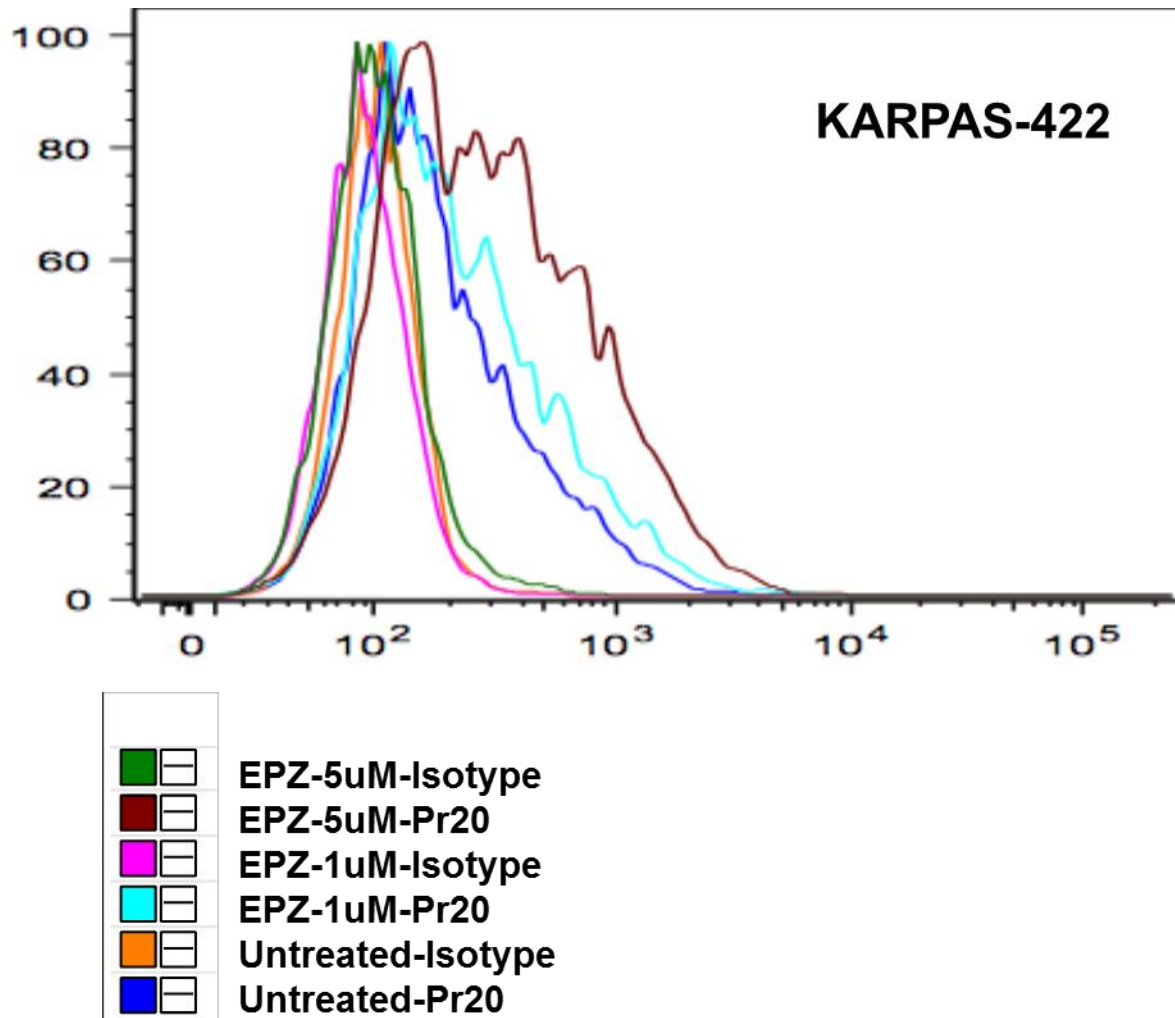


**Figure.S12. Pr20 binding assay in DLBCL cell line.**

Karpas-422 cell line was treated with EPZ-6438 at concentrations of 1uM and 5uM, for 4 days. The cells were harvested, washed and stained with Pr20 mAb or its isotype control hlgG1 conjugated to APC, at a concentration of 3 ug/ml. Data show one of two separate experiments. Both experiments showed binding of Pr20 to the cells, which was enhanced dose-dependently by treating cells with EPZ.

Karpas422  
SU-DHL-4

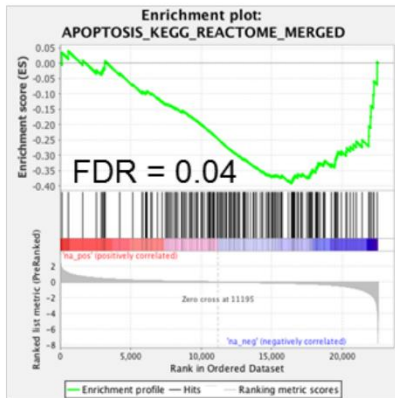


**Figure. S13. Pre-ranked GSEA enrichment plots of apoptosis pathway genes in *PRAME* wt versus *PRAME* KO cell lines.**

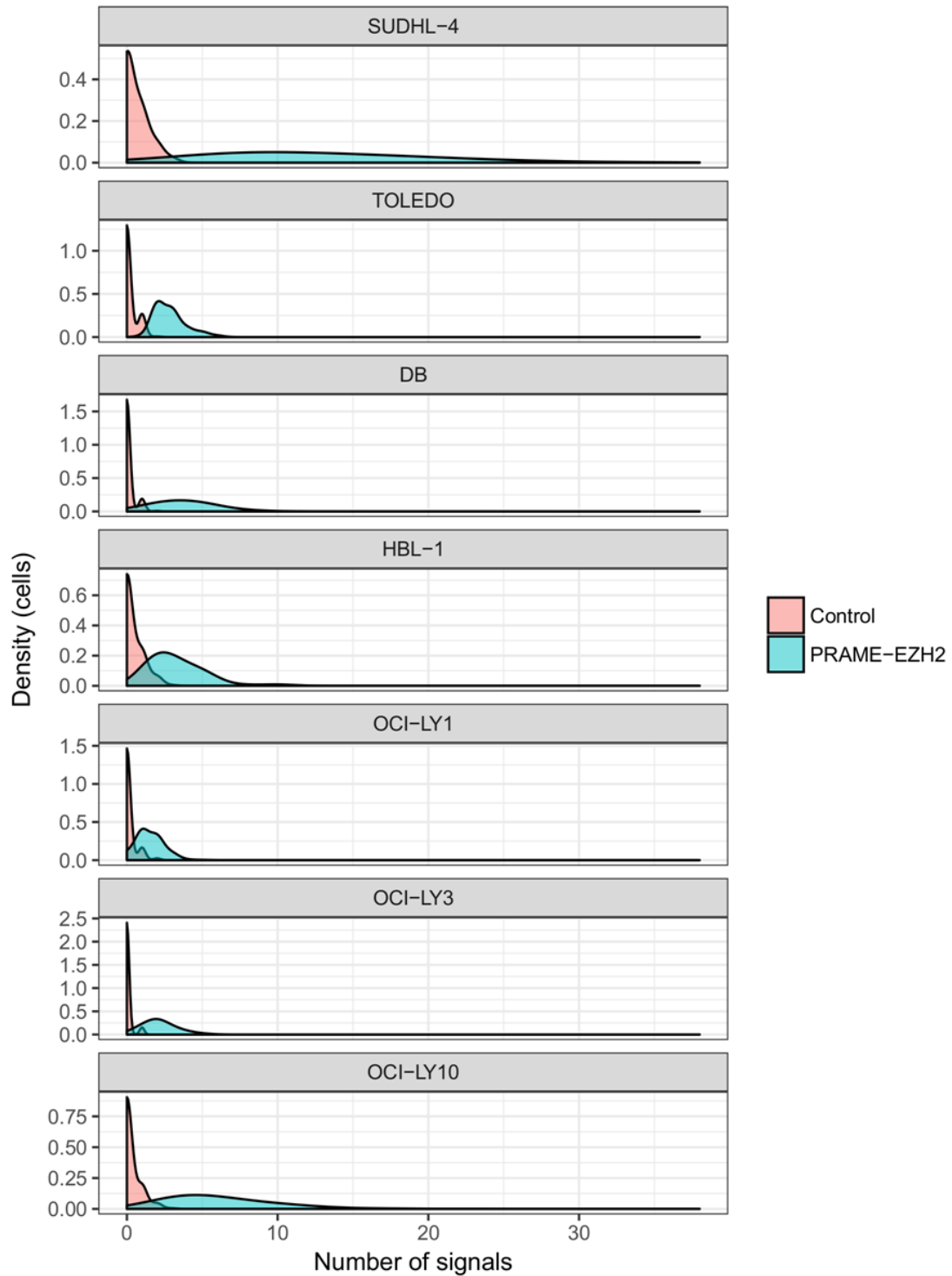


**Figure.S14. PRAME-EZH2 PLA results in each cell line.** Red peak shows control analysis (PRAME antibody/EZH2 antibody only) and blue peak shows EZH2-PRAME combined antibodies.

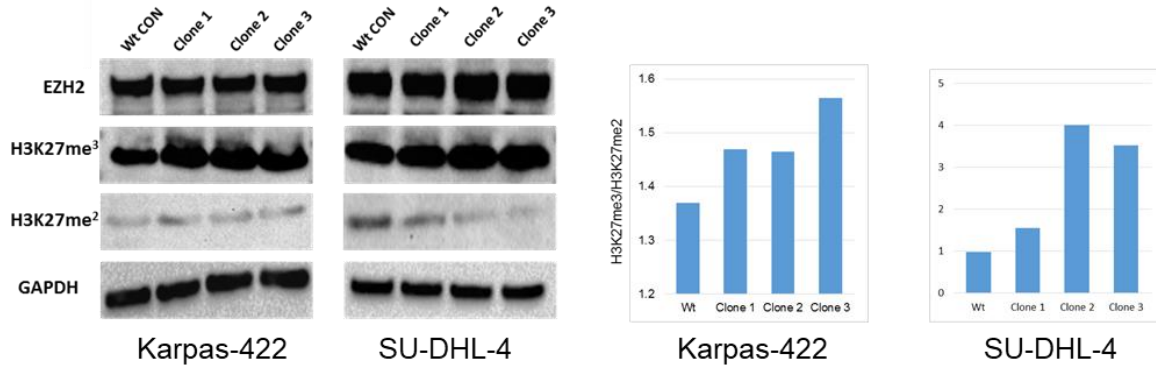


**Figure.S15. EZH2/PRC2 activity change in PRAME isogenic KO cell lines.** Immunoblotting of EZH2, H3K27me3, H3K27me2 in Karpas-422 and SU-DHL-4 isogenic PRAME KO cell lines (left). Densitometry of H3K27me3/H3K27me2 (right). Protein lysate (anti-EZH2, anti-H3K27me3, anti-H3K27me2: 20 $\mu$ g, anti-GAPDH: 5 $\mu$ g) was loaded into separate gels and transferred to separate membranes).